CrystEngComm

www.rsc.org/crystengcomm

Volume 14 | Number 9 | 7 May 2012 | Pages 2983–3322

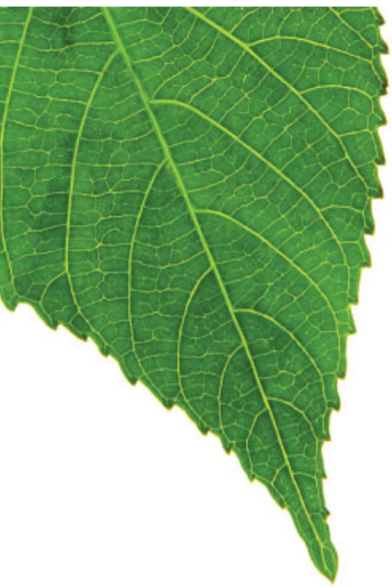

Green Leaf
Red Flower
Clear Water
Enjoy Life

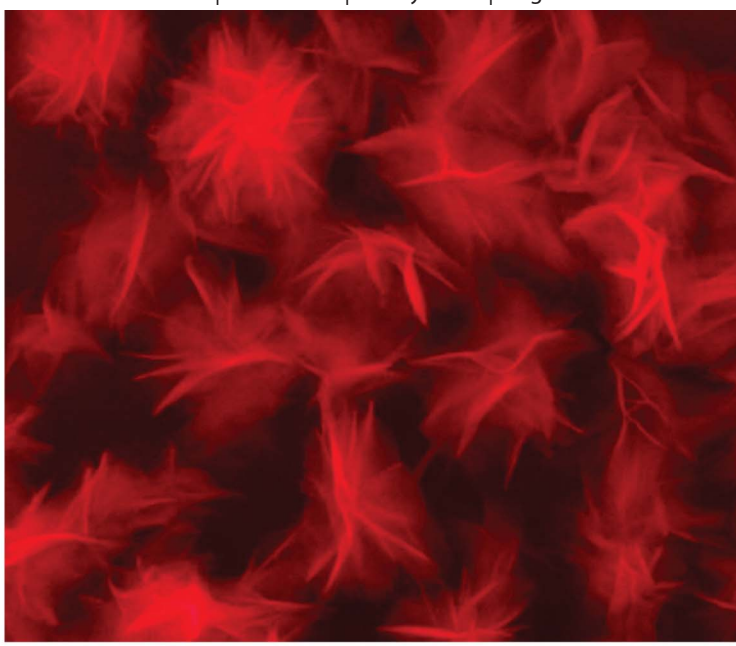

RSC Publishing

COVER ARTICLE

Liu, Huang *et al.*

Self-assembled, monodispersed, flower-like γ-AlOOH hierarchical superstructures for efficient and fast removal of heavy metal ions from water

CrystEngComm

Dynamic Article Links

Cite this: *CrystEngComm*, 2012, **14**, 3005

www.rsc.org/crystengcomm

COMMUNICATION

Self-assembled, monodispersed, flower-like γ-AlOOH hierarchical superstructures for efficient and fast removal of heavy metal ions from water†

Yong-Xing Zhang,[ab] Yong Jia,[b] Zhen Jin,[b] Xin-Yao Yu,[b] Wei-Hong Xu,[b] Tao Luo,[b] Bang-Jing Zhu,[b] Jin-Huai Liu*[ab] and Xing-Jiu Huang*[ab]

Received 18th November 2011, Accepted 11th January 2012
DOI: 10.1039/c2ce06545b

Self-assembled, monodispersed, uniform, and flower-like γ-AlOOH hierarchical superstructures have been synthesized in high yield *via* a simple, economical and environmentally friendly, hydrothermal route. The product possesses a large BET surface area of 145.5 $m^2 g^{-1}$. It is found that Pb(II) and Hg(II) ions can be quickly removed from aqueous solutions by the flower-like γ-AlOOH. After only 5 min, the removal rate for Pb(II) and Hg(II) ions is over 99.0%. The maximal adsorption is *ca.* 124.22 mg g^{-1} for Pb(II) and 131.23 mg g^{-1} for Hg(II).

Heavy metal ions, such as Pb(II), Hg(II), Cd(II), and Cu(II), are highly toxic water pollutants and their efficient removal from water is of great importance. Adsorption is one of the most effective and simplest approaches that has been developed for this purpose. Various metal oxides have been extensively employed as the adsorbents for removing heavy metal ions.[1–3] Among them, γ-Al_2O_3, as a nontoxic and low cost adsorbent, plays an important role in removing heavy metal ions from the natural environment.[4–6] γ-Al_2O_3 can usually be obtained *via* dehydration of γ-AlOOH (boehmite). During heating, the γ-AlOOH nanostructures undergo an isomorphous transformation to nanocrystalline γ-Al_2O_3, and the products can retain the morphology of the parent γ-AlOOH nanostructures.[7] Up to now, various hierarchically structured γ-AlOOH, such as nanowire bunches,[7] hierarchically nanostructured microflowers,[8] rotor-like and carambola-like micro/nanoarchitectures,[9] hollow microspheres,[10] and spindle-like nanoarchitectures,[6] have been prepared. However, it still remains a challenge to develop a facile and environmentally friendly method for obtaining monodispersed, uniform, and flower-like hierarchical γ-AlOOH with thin lamellar structures. In addition, hierarchical γ-AlOOH, as a main precursor for the production of hierarchical γ-Al_2O_3, was also seldom used as an adsorbent for the removal of heavy metal ions (divalent cation) in model wastewater. Herein, we design a simple, economical and environmentally friendly hydrothermal route to synthesize monodispersed, uniform, and flower-like γ-AlOOH at 140 °C for 10 h in high yield, employing deionized water as a solvent and $NaAlO_2$ and urea as reagents in the presence of polyacrylic acid sodium salt (PAAS) as surfactant. In this self-assembly process under hydrothermal conditions, inexpensive aluminium salts and nontoxic reagents were used. The as-obtained flower-like γ-AlOOH structures have a large BET surface area and can be used as adsorbents for the fast removal of highly toxic heavy metal Pb(II) and Hg(II) ions from water. In addition, the product also has a high adsorption capacity for the two metal ions.

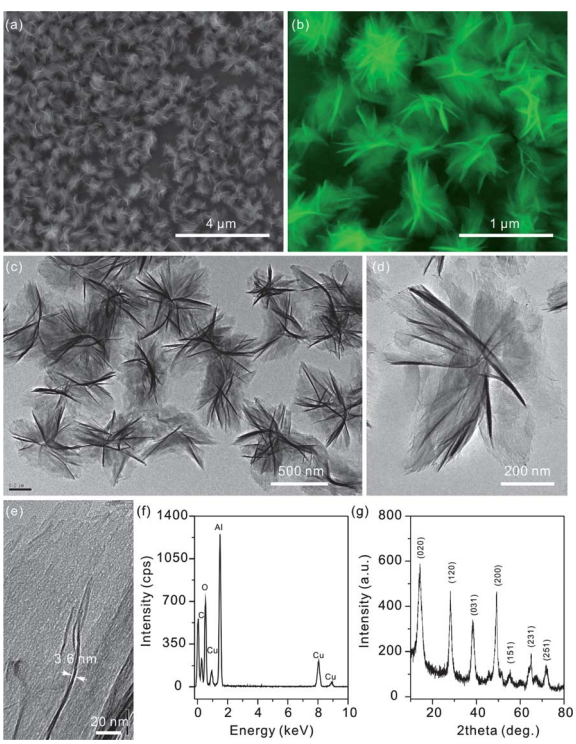

Fig. 1 SEM images (a and b), TEM images (c–e), EDX spectrum (f) and XRD pattern (g) of the flower-like γ-AlOOH.

[a]*Department of Chemistry, University of Science and Technology of China, Hefei, 230026, PR China*
[b]*Research Center for Biomimetic Functional Materials and Sensing Devices, Institute of Intelligent Machines, Chinese Academy of Sciences, Hefei, 230031, PR China. Fax: +86 551 5592420; Tel: +86 551 5591142. E-mail: jhliu@iim.ac.cn; xingjiuhuang@iim.ac.cn*

† Electronic supplementary information (ESI) available: Experimental and synthesis details; complete characterization: FTIR, PL, SEM and XRD. See DOI: 10.1039/c2ce06545b

Scanning electron microscopy (SEM) image of the product (Fig. 1a) shows that the product consists of many monodispersed, uniform, and flower-like architectures with a diameter of approximately 700 nm. The detailed morphology of the flower-like structures is shown in Fig. 2b, which reveal that the structure is composed of many nanosheets with a thickness of 3–8 nm. As-prepared nanoflowers are monodispersed and can be well dispersed in the solution without large aggregation (Fig. 1a and c). The flower-like product is further revealed by the transmission electron microscopy (TEM) images in Fig. 1c and d, from which it is apparent that the structure is assembled by some nanosheets. Fig. 1e reveals the high-resolution TEM images of the nanosheet, which clearly indicate that the nanosheet is a curving lamella with a thickness of *ca.* 3.6 nm. The energy-dispersive X-ray (EDX) spectrum of the nanoflower indicates the presence of Al and O, thereby proving the presence of γ-AlOOH (Fig. 1f). A typical X-ray diffraction (XRD) pattern of the product obtained is shown in Fig. 1g. All of the diffraction peaks can be indexed to the orthorhombic γ-AlOOH (JCPDS 21-1307). Compared with the standard diffraction patterns, no characteristic peaks are from impurities. The Fourier transform infrared spectroscopy (FTIR) spectrum and room temperature photoluminescence (PL) spectrum also confirm the structure of the flower-like γ-AlOOH (see Fig. S1, ESI†).

To investigate the growth mechanism of the flower-like γ-AlOOH, time-dependent experiments were conducted to reveal the growth process. SEM and XRD were employed to monitor the evolution of the morphology and crystalline structure of the products collected at different reaction times. Fig. 2a–d shows the SEM images of the products obtained at different reaction times. As shown in Fig. 2a, after 30 min duration, the product with lamellar morphology appeared. By increasing the hydrothermal time to 1 h, the flower-like product which was assembled by fewer lamellar structures was prepared (Fig. 2b). Further prolonging the reaction to 5 and 10 h, the lamellar structures increased clearly (Fig. 2c and 2d). The morphology of the product did not change with longer reaction time. The corresponding XRD patterns of the intermediate products obtained at different reaction times are shown in Fig. S2 (ESI†). On the basis of the time-dependent experiments, the formation of the flower-like γ-AlOOH can be rationally expressed as a self assembly mechanism as shown in Fig. 2e. First, at high temperature, aluminate anions undergo the following chemical reactions:

$$AlO_2^- + 2H_2O \rightarrow Al(OH)_3 + OH^- \quad (1)$$

$$Al(OH)_3 \rightarrow \gamma\text{-}AlOOH + H_2O \quad (2)$$

When the solution was heated at 140 °C, $Al(OH)_3$ would be formed on the basis of the hydrolysis reaction through eqn (1); the newly formed $Al(OH)_3$ was active and unstable, which would further dehydrate and convert into γ-AlOOH through eqn (2), expectably. Herein, it is noting that PAAS plays a great role in the formation of γ-AlOOH lamellar structures. If there was no PAAS in the reaction system, a product consisting of irregular particles was obtained, as shown in Fig. S3 (ESI†). In our system, PAAS contributed not only to stabilizing and dispersing the γ-AlOOH architectures, but also to controlling the formation of the unique morphologies. According to the literature,[11] oxygen ions are arranged into a distorted octahedral configuration around aluminum in the boehmite lattice and organized in parallel layers linked by hydrogen bonds. In the present work, the hydrogen bonds between the boehmite surface and PAAS molecules reduce the free energy of the crystallites, which bear low-dimentional structures.[12] Hence, the boehmites with sheet-like morphology are observed (Fig. 1e). However, from the thermodynamic point of view, the surface energy of an individual nanosheet is quite high since two main planes are exposed. Thus, the nanosheets tend to aggregate in order to decrease the surface energy by reducing exposed areas.[13] As a result, underdeveloped architectures were formed through oriented self assembly. As the reaction went on, more and more nanosheets were assembled together to form flower-like structures. In addition, the product morphology is also sensitive to the temperature of the reaction process. The detailed results and discussion are shown in Fig. S4 (ESI†).

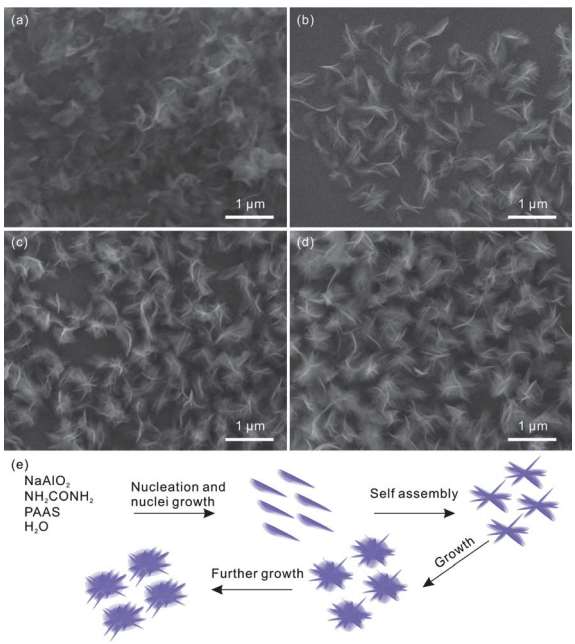

Fig. 2 SEM images of the products collected at different reaction times. (a) 0.5 h, (b) 1 h, (c) 5 h, (d) 10 h, (e) schematic illustration of the morphological evolution process of the as-obtained γ-AlOOH.

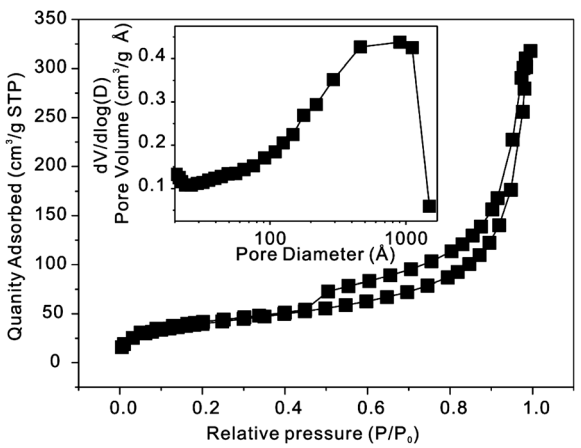

Fig. 3 Nitrogen adsorption/desorption isotherm and BJH pore size distribution plot (inset) of the flower-like γ-AlOOH.

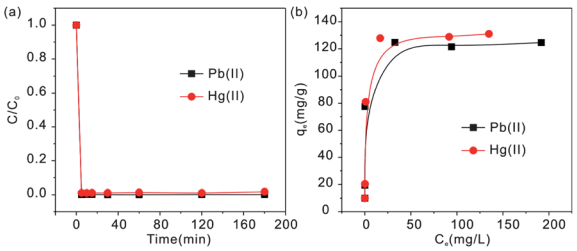

Fig. 4 (a) Time-dependent concentration of Pb(II) (initial concentration of 73.9 mg L^{-1}) and Hg(II) (initial concentration of 82.0 mg L^{-1}) using flower-like γ-AlOOH. (b) Adsorption isotherms of Pb(II) and Hg(II) using flower-like γ-AlOOH.

Nitrogen adsorption and desorption isotherm measurements were conducted to investigate the structure of the flower-like γ-AlOOH. As shown in Fig. 3, the BET surface area and the pore volume have been estimated to be 145.5 $m^2 g^{-1}$ and 0.396 $cm^3 g^{-1}$, respectively. The pore size distribution curve of the product exhibits a broad peak in the range of 10–100 nm with a maximum at 90 nm. The result indicates that there are some mesopores/macropores in the flower-like γ-AlOOH. The mesopores reflect porosity between the nanosheets which formed the flowerlike γ-AlOOH, while larger mesopores/macropores can be related to the pores formed between the flowerlike γ-AlOOH. These mesoporous/macroporous structures can be also directly observed from the SEM and TEM images of the product shown in Fig. 1. The high BET surface area, high value of pore volume and ideal pore size distribution made the flower-like γ-AlOOH a promising candidate for application in heavy metal ion removal from water. As is well known, Pb(II) and Hg(II) are considered to highly toxic water pollutants, and their efficient removal from water is of great importance. Herein, we investigated the capacity of the flower-like γ-AlOOH to remove Pb(II) and Hg(II) ions from aqueous solutions. From Fig. 4a, it is clear that over 99.0% of the heavy metal ions had been adsorbed at room temperature after only 5 min. The relationship between the removal ability of the material and the concentration of the heavy metal ion solution could be illustrated by an adsorption isotherm. Fig. 4b shows the adsorption isotherms of Pb(II) and Hg(II) for the flower-like γ-AlOOH. The Langmuir adsorption model was employed for the adsorption analysis. Such a model was used to represent the relationship between the amount of heavy metal adsorbed at equilibrium (q_e, mg g^{-1}) and the equilibrium solute concentration (C_e, mg L^{-1}),[14] $q_e = q_m K_L C_e/(1 + K_L C_e)$, where q_m (mg g^{-1}) is the maximum adsorption capacity and K_L (L mg^{-1}) is the equilibrium constant. The maximal adsorption of the flower-like γ-AlOOH is *ca.* 124.22 mg g^{-1} for Pb(II) and 131.23 mg g^{-1} for Hg(II). These values are much higher than those from microsphere-like γ-AlOOH which was prepared without PAAS (the maximum adsorption capacity is *ca.* 50.61 mg g^{-1} for Pb(II) and 55.22 mg g^{-1} for Hg(II)) and other hierarchical structure adsorbents[15–18] reported earlier, and about 6 times higher than that of activated carbon.[19] Heavy metal ion adsorption by metal oxide is likely from the combination of static electrical attraction between oxides and heavy metal ions and ion exchange in the aqueous solution.[14] The monodispersed, hierarchical structure with the large number of OH groups on the surface of thin lamellar structures, high BET surface area and porous structure should be the critical factors for the fast removal rate and high adsorption capacity of the γ-AlOOH.

In summary, self-assembled, monodispersed, uniform, and flower-like γ-AlOOH has been successfully synthesized *via* a simple, economical and environmentally friendly, hydrothermal route. The reaction mechanism and the self-assembly evolution process were studied. The product possesses a large BET surface area of 145.5 $m^2 g^{-1}$. It is found that Pb(II) and Hg(II) ions can be quickly removed from aqueous solutions by the flower-like γ-AlOOH. After only 5 min, the removal rate for Pb(II) and Hg(II) ions is over 99.0%. The maximal adsorption is *ca.* 124.22 mg g^{-1} for Pb(II) and 131.23 mg g^{-1} for Hg(II). All of these splendid properties mean that the product can be used as a highly efficient sorbent for the removal of heavy metal ions from waste water.

This work was supported by the One Hundred Person Project of the Chinese Academy of Sciences, the National Key Scientific Program, Nanoscience and Nanotechnology (Grant No. 2011CB933700).

Notes and references

1 L. J. Wan, L. S. Zhong, J. S. Hu, H. P. Liang, A. M. Cao and W. G. Song, *Adv. Mater.*, 2006, **18**, 2426–2431.
2 L. J. Wan, L. S. Zhong, J. S. Hu, A. M. Cao, Q. Liu and W. G. Song, *Chem. Mater.*, 2007, **19**, 1648–1655.
3 L. J. Wan, L. S. Zhong, J. S. Hu and W. G. Song, *Chem. Commun.*, 2008, 1184–1186.
4 C. H. Wu, C. F. Lin, H. W. Ma and T. Q. Hsi, *Water Res.*, 2003, **37**, 743–752.
5 Y. Q. Wang, G. Z. Wang, H. Q. Wang, W. P. Cai, C. H. Liang and L. Zhang, *Nanotechnology*, 2009, **20**, 155604.
6 W. Q. Cai, J. G. Yu and M. Jaroniec, *J. Mater. Chem.*, 2010, **20**, 4587–4594.
7 C. C. Tang, J. Zhang, S. Y. Wei, J. Lin, J. J. Luo, S. J. Liu, H. S. Song, E. Elawad, X. Ding, J. M. Gao and S. R. Qi, *J. Phys. Chem. B*, 2006, **110**, 21680–21683.
8 W. J. Zheng, T. Kim, J. B. Lian, J. M. Ma and X. C. Duan, *Cryst. Growth Des.*, 2010, **10**, 2928–2933.
9 Y. Z. Yang, H. Liang, L. Liu, H. X. Yang, J. J. Wei and Z. J. Yang, *CrystEngComm*, 2011, **13**, 2445–2450.
10 W. Q. Cai, J. G. Yu and S. Mann, *Microporous Mesoporous Mater.*, 2009, **122**, 42–47.
11 A. C. Pierre and D. R. Uhlmann, *J. Non-Cryst. Solids*, 1986, **82**, 271–276.
12 W. Q. Cai, H. Q. Li and Y. Zhang, *Mater. Chem. Phys.*, 2006, **96**, 136–139.
13 Y. J. Zhu, L. X. Yang, H. Tong, Z. H. Liang and W. W. Wang, *Cryst. Growth Des.*, 2007, **7**, 2716–2719.
14 J. H. Qu, R. C. Wu and Y. S. Chen, *Water Res.*, 2005, **39**, 630–638.
15 Y. H. Ni, K. Mi, C. Cheng, J. Xia, X. Ma and J. M. Hong, *Chem. Commun.*, 2011, **47**, 5891–5893.
16 L. Yang, F. F. Wang, Y. M. Guo, H. J. Wang, K. Wang, X. M. Ma, W. G. Yao and H. Zhang, *CrystEngComm*, 2011, **13**, 5634–5637.
17 Y. H. Ni, L. N. Jin, L. Zhang and J. M. Hong, *J. Mater. Chem.*, 2010, **20**, 6430–6436.
18 Y. H. Ni, K. M. Liao and J. Li, *CrystEngComm*, 2010, **12**, 1568–1575.
19 M. A. Ferrogarcia, J. Riverautrilla, I. Bautistatoledo and M. D. Mingorance, *Carbon*, 1990, **28**, 545–552.